JACS
JOURNAL OF THE AMERICAN CHEMICAL SOCIETY
Article
pubs.acs.org/JACS

Metal–Sulfur Battery Cathodes Based on PAN–Sulfur Composites

Shuya Wei,[†] Lin Ma,[‡] Kenville E. Hendrickson,[†] Zhengyuan Tu,[‡] and Lynden A. Archer*[,†]

[†]School of Chemical and Biomolecular Engineering, [‡]Department of Materials Science and Engineering, Cornell University, Ithaca, New York 14853, United States

Supporting Information

ABSTRACT: Sulfur/polyacrylonitrile composites provide a promising route toward cathode materials that overcome multiple, stubborn technical barriers to high-energy, rechargeable lithium–sulfur (Li–S) cells. Using a facile thermal synthesis procedure in which sulfur and polyacrylonitrile (PAN) are the only reactants, we create a family of sulfur/PAN (SPAN) nanocomposites in which sulfur is maintained as S_3/S_2 during all stages of the redox process. By entrapping these smaller molecular sulfur species in the cathode through covalent bonding to and physical confinement in a conductive host, these materials are shown to completely eliminate polysulfide dissolution and shuttling between lithium anode and sulfur cathode. We also show that, in the absence of any of the usual salt additives required to stabilize the anode in traditional Li–S cells, Li–SPAN cells cycle trouble free and at high Coulombic efficiencies in simple carbonate electrolytes. Electrochemical and spectroscopic analysis of the SPAN cathodes at various stages of charge and discharge further show a full and reversible reduction and oxidation between elemental sulfur and Li-ions in the electrolyte to produce Li_2S as the only discharge product over hundreds of cycles of charge and discharge at fixed current densities.

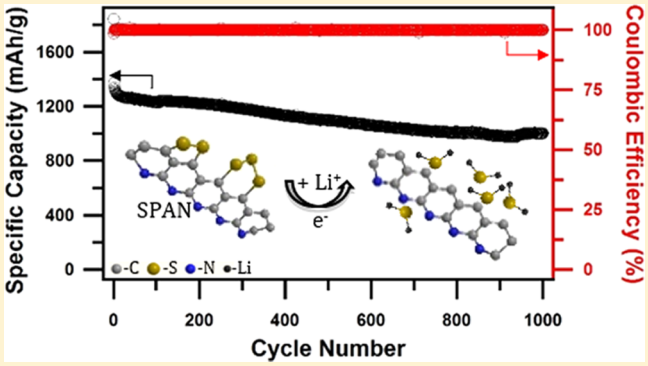

INTRODUCTION

Electrochemical storage technologies that offer higher specific capacity, improved safety, and extended performance lifetimes have received intensive consideration during the past decade to meet rising standards for portable electronic devices, electric vehicles, and high-performance autonomous aircraft and robotics. Rechargeable electrochemical cells that use earth-abundant and low-cost materials are understood to be particularly good candidates to achieve many of these performance goals and may also offer other attractive attributes, such as environmental benignity and scalability.[1−4] Among all solid-state cathodes, elemental sulfur offers the greatest promise for reversibly storing large amounts of electrical energy, up to 2.5 kWh/kg or 2.8 kWh/L, at moderate cost.[3,5] Unlike currently used lithium-ion (Li-ion) batteries, which are based on intercalation chemistries in the cathode that yield one or fewer than one electron per transition metal ion,[6] a lithium–sulfur (Li–S) cell takes advantage of the spontaneous and reversible conversion reaction of sulfur with lithium ions in the cathode to ideally form lithium sulfide (Li_2S). The high energy of these cells derives from the fact that the conversion reaction yields up to two electrons per sulfur atom (1675 mAh/g) at a potential of around 2.1 V.[7−9]

The superficial simplicity of the electrochemistry in the Li–S cell belie multiple challenges stemming from the complicated solution phase thermodynamics of sulfur and its reduction products in the cathode as well as the resultant poor transport of electrons and ions in the Li–S battery electrodes and electrolyte. The insulating nature of sulfur and sulfides, for instance, limits electron transport in the cathode and leads to low active material utilization. Sulfur electrodes also have low stability due to the formation of soluble lithium polysulfides (LiPS) during the reduction of sulfur with lithium. In particular, the high solubility of intermediate LiPS species in commonly used electrolytes and its reactivity with others causes loss of active material. Dissolved LiPS may also diffuse in the electrolyte, which increases its viscosity, lowers ionic conductivity, may clog the separator membrane, and may react with the metallic lithium anode in a parasitic, cyclic process termed shuttling, which not only leads to Li–S cell performance well below expectations for this chemistry but also to degradation in performance over time.[7,8,10,11] Thus, unlike the traditional Li-ion batteries, where cell-level performance usually approaches 90% of theoretical capacities set by the chemistry of the anode and cathode, the best performing Li–S cells rarely deliver storage capacities above 60% of theoretical value.[9]

Herein, we report a facile synthesis scheme, chemistry, and electrochemical properties of a family of sulfur/polyacrylonitrile (SPAN) composites that utilize specific interactions with nitrile groups on the polymer backbone and S_8 to destabilize PAN and to promote dehydrogenation and ring formation (Scheme 1). Thermal treatment of the material is shown to lead to metastable, covalently bound sulfur species S_x (x = 2–3) that

Received: May 22, 2015
Published: September 1, 2015

DOI: 10.1021/jacs.5b08113
J. Am. Chem. Soc. 2015, 137, 12143−12152

Scheme 1. Proposed Synthesis Route for Creating Sulfur/Polyacrylonitrile (SPAN) Nanocomposite Cathode Materials

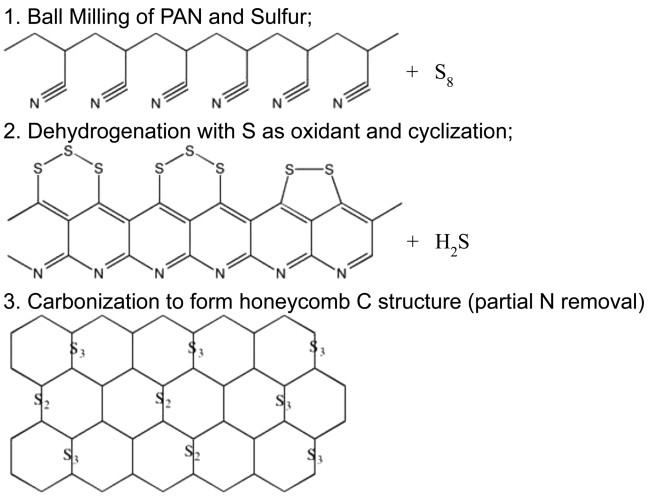

are integrated throughout the composite.[12] The approach builds on the two most successful strategies, physical confinement and chemical sequestration, reported for improving electrochemical activity of sulfur in Li−S cells. Cathodes based on porous carbonaceous materials, for example, have been proposed previously for physically trapping LiPS and improving electronic transport.[3,13−16] Of these approaches, microporous carbon materials are thought to provide the strongest physical confinement/immobilization of sulfur and its reduction products due to extremely small pore sizes. Notably, cyclic voltammetry analysis of cells based on this cathode design have been reported to exhibit an absence of the higher (2.35 V) reduction process associated with formation of high-order LiPS by reaction of Li^+ and S_8 and subsequent loss of LiPS to the electrolyte.[17−19] This implies that in such cathodes sulfur may exist in forms other than S_8. Xin, for example, has argued in favor of smaller S_x (x = 2−4) molecules that upon reduction with Li^+ cannot form soluble high-order LiPS.[18] Although this argument is a reasonable interpretation of the electrochemistry data, support from thermodynamic analysis of the electrode has been lacking so far.

Various approaches for chemically sequestering LiPS, by affinity particles/molecules/functional groups incorporated as additives in the sulfur cathode, also have been studied with differing degrees of success. Graphene oxide, metal oxides (SiO_2, TiO_2, V_2O_5, Al_2O_3, TiS_2) particles, and nitrogen-doped polymers such as polypyrrole, polyaniline, and polyacrylonitrile (PAN),[12,20−28] for instance, all have been used as additives or protective coating layers, where the high binding energy between LiPS and O,N-containing molecules is thought to be beneficial. Guo et al. have provided the most direct evidence in support of this concept by showing that addition of soluble LiPS to stable PAN/dimethylformamide (DMF) solutions led to rapid gel formation, in which PAN chains swollen by DMF are cross-linked by LiPS.[29] The strong affinity between LiPS and nitrile-containing molecules also has been confirmed recently both by density functional theory and diffusion experiments.[30] An important result from the study by Guo et al. is that sulfur species associated with nitrile groups in the cross-linked polymer solutions remain well-dispersed in carbon materials derived from the PAN component, by first removing the DMF solvent and pyrrolizing the PAN in an inert environment. A key conclusion from this study is that when proper attention is given to removing physically adsorbed S_8 a similar process leads to the spontaneous formation of S_2 and S_3 species linked to a conductive, PAN-derived carbon framework.

SPAN composites have attracted recent interest as cathode materials for Li−S batteries due to the opportunities they appear to offer for employing both of the approaches discussed above.[12,20,31−34] In 2002, Wang and co-workers appear to be the first to report that SPAN composites possess good enough charge and ion transport properties to be used as cathodes in rechargeable lithium batteries.[20] Although the composite cathode exhibited good stability in electrochemical cycling studies, no evidence of C−S bonds was observed from FTIR studies, suggesting that sulfur exists mainly in elemental form. Fanous et al. used TOF-SIMS to characterize SPAN composites subjected to different thermal synthesis protocols and report CNS-fragments in the materials treated at elevated temperature.[12] Hwang et al. recently reported that these SPAN composites processed in a fiber morphology exhibit good electrochemical stability when employed as cathodes for sodium−sulfur cells.[33] There have been numerous follow-on-type studies of electrochemical properties of this composite; however, the electrochemical lithiation and delithiation processes are still largely unknown. The details of how sulfur interacts with the conductive polymeric host material during charging and discharging are understood to be important, but, so far, this has been scarcely studied. In this work, we report on the thermal synthesis of sulfur/PAN nanocomposites and employ electrochemical and spectroscopic tools to evaluate various hypotheses (Scheme 2) for lithiation and delithiation processes in these materials.

Scheme 2. Proposed Lithiation Mechanisms for SPAN Nanocomposites[a]

Reaction 1:	$RSSR+2Li^+ \leftrightarrow 2RSLi$
Reaction 2:	$RSSSR+4Li^+ \leftrightarrow 2RSLi+Li_2S$
Reaction 3:	$RSSR+4Li^+ \leftrightarrow 2R+2Li_2S$
Reaction 4:	$RSSSR+6Li^+ \leftrightarrow 2R+3Li_2S$

[a]RSSR, RSSSR: organosulfur-based materials.

Reactions 1 and 2 assume that S−S linkages that covalently bond to organic polymer materials can reversibly cleave and reform by analogous redox chemistry to that reported for thiolates (RS^-).[24,35,36] It is known that these reactions involve one-electron transfer per sulfur atom, which gives a theoretical specific capacity of 837 mAh/g_S. In Reactions 3 and 4, the R−S bond completely breaks during the lithiation process, resulting in the formation of Li_2S as the only sulfur-containing lithiation product. This reaction involves two-electron transfers per sulfur atom, yielding a theoretical capacity of 1675 mAh/g_S.

RESULTS AND DISCUSSION

The specific synthesis route used in the study is shown in Scheme 1 and detailed in the experimental section (see Supporting Information). Briefly, to prepare SPAN, a simple

DOI: 10.1021/jacs.5b08113
J. Am. Chem. Soc. 2015, 137, 12143−12152

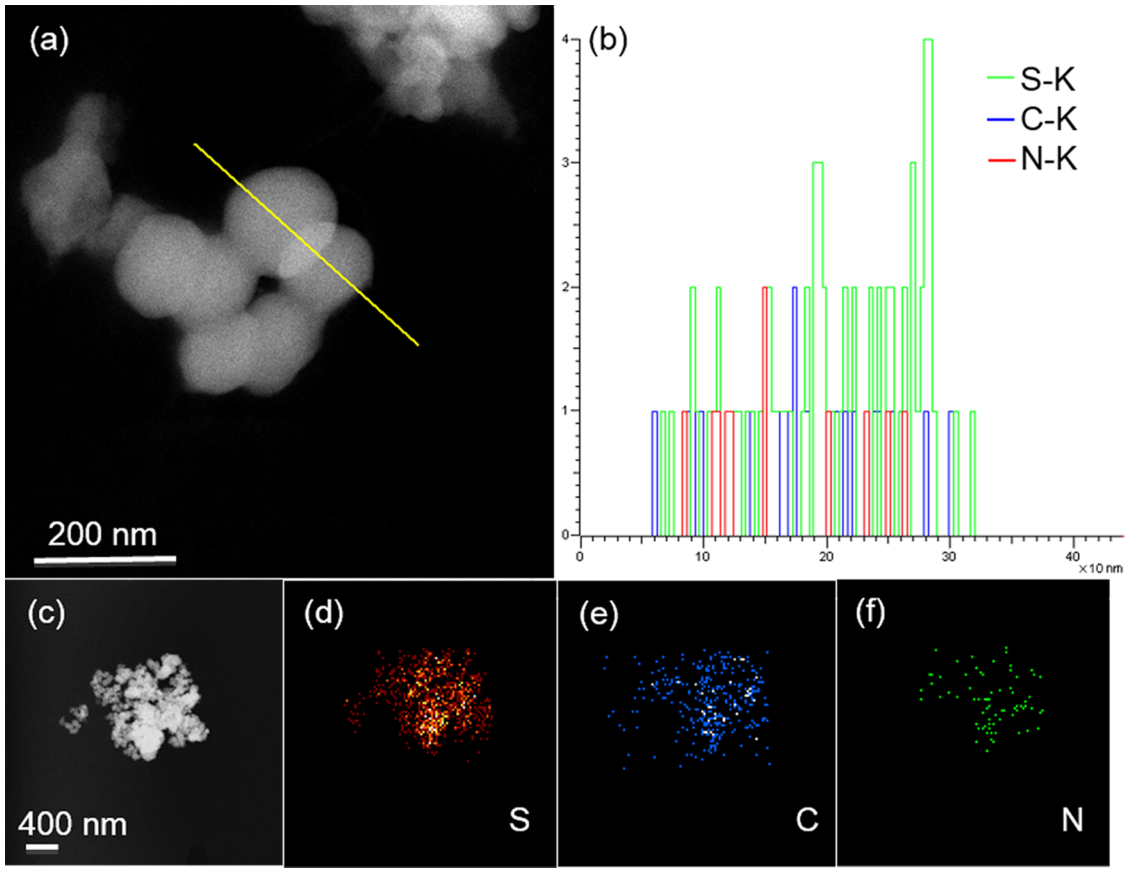

Figure 1. STEM (a, c) images of the SPAN4 composite; EDX sulfur (d), carbon (e), and nitrogen (f) maps based on the area shown in (c); and (b) normalized EELS intensity along the line in (a).

one-step procedure was employed involving thermal treatment of physical PAN/sulfur blends at a low temperature ramp rate of 5 °C/min and under continuous nitrogen gas flow. In the following sections, materials prepared using thermal treatment of the blends at 250, 350, 450, and 600 °C are denoted SPAN2, SPAN3, SPAN4, and SPAN6, respectively. As a control, PAN without sulfur was heat-treated at 450 °C and is denoted PANC. It is believed that cyclization of the polymer backbone carbons is facilitated by sulfur coordination with and subsequent cleaving of the CN triple bonds. It is further hypothesized that cyclic sulfur (S_8) is, in the process, cleaved into smaller chain sulfur radicals, which are able to react with and covalently bond to the PAN carbon backbone and dehydrogenate the material to form H_2S. A similar scheme for the dehydrogenation and cyclization of PAN in the presence of sulfur has been reported previously.[12,21,37,38] At high temperature, PAN may further carbonize to produce pyridinic-N carbon ring structures encapsulating sulfur species.

Figure 1a,c reports typical STEM images for as-synthesized SPAN4. The figure indicates that the material exists in a nanosphere morphology with average diameters between 100 and 150 nm, which is consistent with results deduced from scanning electron microscopy (SEM) images (Figure S1, Supporting Information). Similar structures have been reported in previous studies.[20,32,37] To determine the distribution of S, N, and C in SPAN4, energy dispersive X-ray (EDX) maps based on the area shown in the annular dark field (ADF) image (Figure 1c) reveals that SPAN4 contains 45.6% sulfur. This composition is higher than that in previous literature reports,[21,33] and we attribute it to the low thermal ramp rates used in the pyrolysis step. The sulfur and carbon maps in Figure 1d,e match the result shown in the ADF image (Figure 1c), indicating that carbon and sulfur are homogeneously distributed throughout the materials. The nitrogen map (Figure 1f) shows that SPAN4 contains 8.59% N, indicating only partial removal of N atoms during heat treatment. Electron energy loss spectroscopy (EELS) was performed on the composite to investigate the distribution of elements along the line shown in Figure 1a. Figure 1b reports the normalized EELS intensities with respect to position for the S-K, C-K, and N-K edges. The results show more sulfur intensity along the middle of the line, indicating that sulfur is most probably encapsulated by carbon rings.

The thermal stability of the various SPAN materials, PANC, and PAN is assessed by thermal gravimetric analysis (TGA) in the temperature range from 25 to 1000 °C (Figure S2). SPAN2 exhibits a significant weight loss of 42% in the range 200 and 400 °C, which is ascribed to sublimation of unreacted elemental sulfur. For the other SPAN materials, more significant and distinctive weight loss is observed at much higher temperature, beyond 500 °C. It reflects the strong bonding between carbon and sulfur and is consistent with the higher dissociation energy of the C−S (272 kJ/mol) bond compared to that of the S−S bond (251 kJ/mol).[33] XRD analysis (Figure S3) reveals that sulfur in the orthorhombic S_8 state exists only in SPAN2, the material synthesized at the lowest temperature; no sulfur peaks can be observed in any of the other SPAN materials, suggesting that the sulfur embedded at higher temperatures loses all crystallinity. A broad diffraction peak at $2\theta = 26.5°$ corresponding to the graphitic (002) plane is also apparent in

DOI: 10.1021/jacs.5b08113
J. Am. Chem. Soc. 2015, 137, 12143−12152

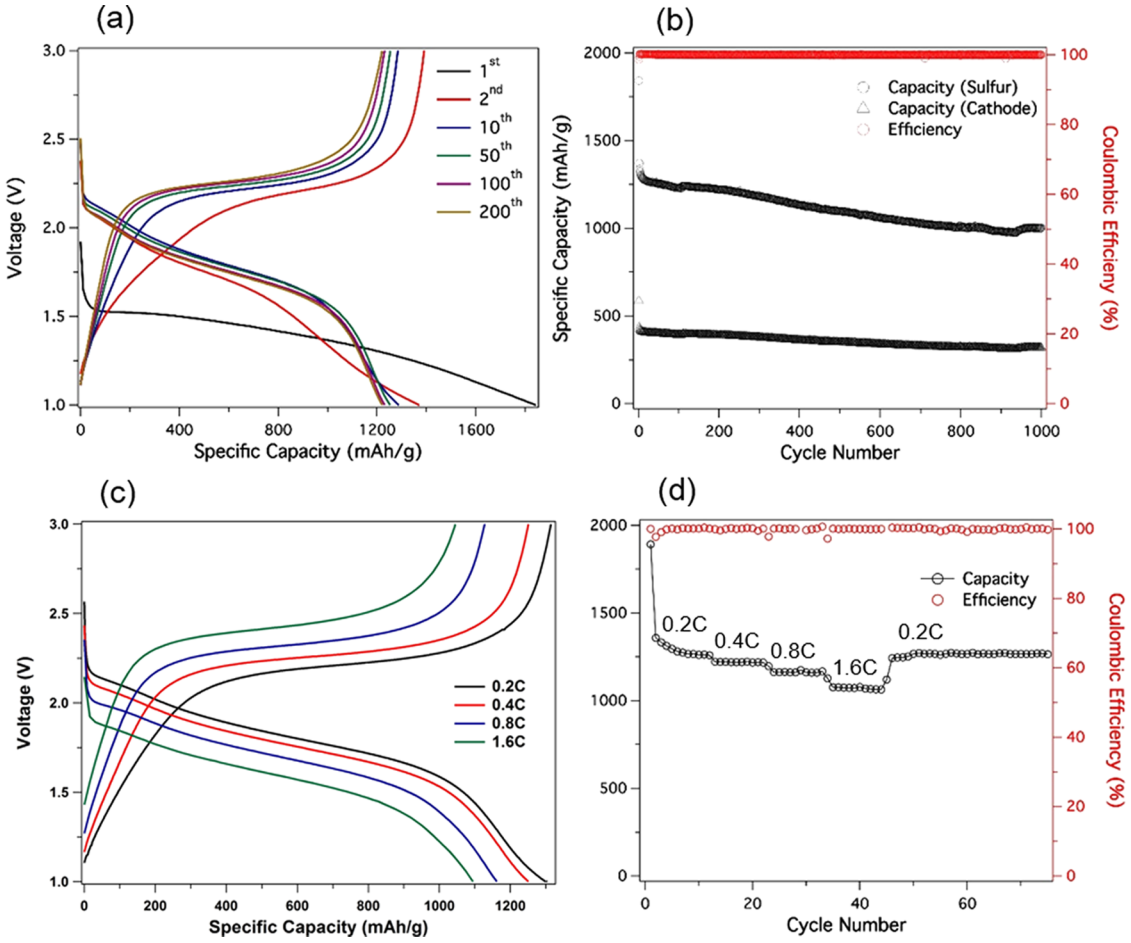

Figure 2. (a) Electrochemical discharge and charge curves of SPAN4 at various cycles. The tests were performed at 0.4 C for both charge and discharge in the potential range of 1−3 V vs Li/Li^+. (b) Capacity and Coulombic efficiencies versus cycle number for PANS4. The black circles report capacities relative to the weight of the active sulfur species in the cathode, whereas the data represented by black triangles are the corresponding capacities based on the overall cathode mass. (c, d) Rate performances of the SPANS measured at various C-rates. The C-rates were same for both charge and discharge in each cycle.

the SPAN materials, verifying the carbonization of PAN. A signature peak at $2\theta = 17°$, corresponding to the (110) plane of the PAN crystal, completely disappears after carbonization with sulfur. To analyze the chemical structure of the SPANs, Raman (Figure S4a) and FTIR (Figure S4b) spectra for composites were performed, with PANC, PAN, and sulfur used as controls. Specific peak assignments are summarized in Tables S1 and S2 of the Supporting Information. On the basis of the information, the structure of the SPAN can be confirmed to be a turbostratic carbon configuration via dehydrogenation and efficient $\pi-\pi$ stacking, with sulfur covalently bonded to the carbon backbone.[21,32,33]

Electrochemical characteristics of the SPAN composites were characterized in 2032 coin cells with the composite as the active cathode material and lithium foil as the counter electrode. We studied SPAN4 in detail, as it exhibited superior electrochemical properties among all of the SPAN materials as well as acceptable sulfur content. To illustrate, the first discharge voltage profile for different SPAN-based cathodes is shown in Figure S5a. It is seen that the discharge voltage plateau decreases with an increase in the preparation temperature for the SPANs. However, the sulfur content in the materials generally decreases as the temperature increases; thus, there is a clear trade-off between sulfur content and binding strength between S and C atoms, with optimal results for both features of the materials found in SPAN4. Two types of electrolytes, 1 M $LiPF_6$ in EC/DEC and 1 M LiTFSI in DOL/DME with $LiNO_3$ as additive, were used in the study to assess the electrodes. This assessment revealed unexpected results that appear to be critical for understanding the chemistry of the SPAN4 material and the exceptional electrochemical properties of sulfur cathodes based on this material. Figure 2a reports the galvanostatic charge/discharge profile in a cell cycled in the former electrolyte. Comparison of the discharge profiles between the second and 200th cycles reveals negligible changes in both the shape and specific capacity. Figure 2b shows that the material exhibits exceptionally stable cycling stability for over 1000 cycles at 0.4 C (1 C = 1675 mA/g) based on sulfur. The capacity degradation/fade upon repeated cycles of discharge and charge is only 0.027% per cycle from the second to 1000th cycle. The figure also shows that SPAN4 delivers a capacity of over 1000 mAh/g even after 1000 cycles. Although Wang reported an even higher capacity of 1630 mAh/g for a Li−S cell, the current density used in that study was much lower (0.012 C).[39]

Figure 2a shows that the voltage plateau during the first discharge cycle (~1.5 V) is lower than the values observed in subsequent cycles. This implies that the reduction reaction and transport in the cathode involve different processes, probably cleavage of S−S bonds in the composite, compared to those in

DOI: 10.1021/jacs.5b08113
J. Am. Chem. Soc. 2015, 137, 12143−12152

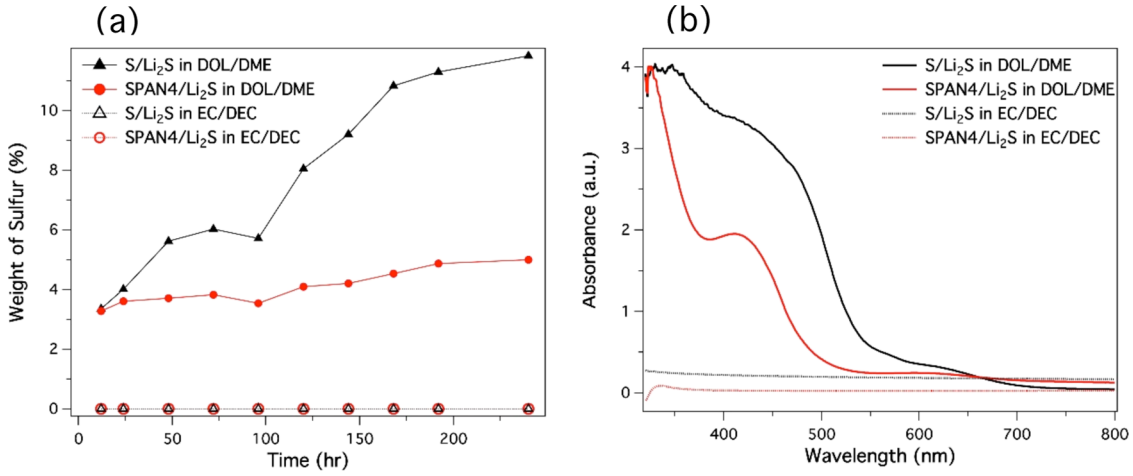

Figure 3. (a) Sulfur content in the electrolyte for four different cases; (b) UV−vis spectra of the solutions for the four samples after 10 days, which are equally diluted with the corresponding electrolyte.

subsequent cycles. The capacity (1843 mAh/g_{sulfur}) estimated for the initial discharge is higher than the theoretical capacity of sulfur. This means that the π-conjugated pyridinic carbon framework likely makes a contribution, probably a combination of Faradaic processes in forming the solid−electrolyte interlayer (SEI) on carbon during the first cycle and a non-Faradaic pseudocapacitance that may persist over many cycles.[24] The voltage profile of a Li−S cell containing PANC, without sulfur, as a control cathode is shown in Figure S5b. Although the material has a low degree of ordered graphitic structure compared to that of SPAN, it still evidently possesses about 5% of the storage capacity of the SPAN4 cathode during the first cycle. During the following cycles of discharge, the voltage plateau increases and remains stable between 1.6 and 2.1 V over hundreds of cycles of charge and discharge. This observation is evidently distinct from what is typically found in Li−S cells, where a two-step discharge plateau is observed. In the first step at ∼2.35 V, the plateau is associated with the reaction of Li^+ and S_8 to form LiPS. The second plateau at ∼2.1 V is attributed to reversible reactions between smaller sulfur species (e.g., LiS_3 and Li_2S_3).[40−42] The fact that only the latter of these two voltage plateaus is observed in electrodes based on SPAN4 is significant because it means that in the material sulfur exists in a form that prevents it from achieving its bulk thermodynamically favored form, S_8, even when the Li−S cells are in the fully charged state. The result is also significant because it means that LiPS cannot form in these cells, which eliminates complications such as shuttling associated with formation and dissolution of LiPS in the electrolyte. The plausibility of this conclusion will be supported more fully in the sections to follow; however, the high Coulombic efficiencies evident in Figure 2b over extended cycling of the cells, without any of the usual $LiNO_3$ additive in the electrolyte, provide additional proof that shuttling has been arrested in this cathode design. Figures 2c,d reports the effect of current density on performance of Li−S cells that utilize a SPAN4 cathode. Current densities from 0.08 mA/cm^2 (=0.2 C) to 0.63 mA/cm^2 (=1.6 C) were investigated. In each cycle, the rates were the same for both charge and discharge. The similarity of the charge and discharge profiles, irrespective of rate, is clearly apparent from the figures. As illustrated in Figure 2d, the SPAN4 cell also shows high capacity retention at different C-rates, with an average of only 4.13% capacity decay through high C-rate (1.6 C) to low C-rate (0.4 C). Importantly, once the C-rate is reduced to the original value of 0.2 C, the capacity recovers to its previous steady value.

Reaction of sulfur with PAN at high temperature is expected to produce S_x cross-links covalently linked to the carbon rings.[12] After the initial discharge, however, the S−S bond may be expected to break and, upon cell recharge, any sulfur species present in the cathode may spontaneously transform into high-order LiPS and S_8, which would remove the benefits of covalently linking the sulfur to carbon in the cathode.[11] The absence of the characteristic 2.35 V discharge plateau after hundreds of discharge cycles of the SPAN4 cathode is somehow able to avoid this fate. Moreover, the charge and discharge profiles are more symmetric compared to those of Li−S cells made with elemental sulfur as cathodes, which again indicates that there is excellent utilization of sulfur in the cathode and very little if any losses to the electrolyte.

The inability of unbound smaller sulfur species produced in the cathode after the first recharge to transform to S_8 and, in the subsequent discharge, to LiPS implies that the smaller sulfur species are perhaps isolated/encapsulated in the cathode. To understand the nature of the interactions that hold the smaller sulfur species in the cathode, we compared the electrochemical behavior of cells in which the commonly used 1 M LiTFSI in DOL/DME with and without $LiNO_3$ (Figure S6) electrolyte is substituted for the 1 M $LiPF_6$ in EC/DEC electrolyte used in the studies reported in Figure 2. It is apparent that this change has dramatic and negative consequences on cell performance. Specifically, while the discharge profile and specific capacity for the first discharge cycle are comparable for SPAN4 cycled in the two electrolytes, it is clear that by the second cycle a two-step discharge profile, analogous to what is seen in a conventional Li−S cell, is observed and that this is accompanied by shuttling and significant deterioration in cell performance upon charging. Even if Guo et al.[29] used solid Li_2S encapsulated in PAN as cathode, a two-step discharge plateau is still observed in a LiPS-soluble tetraethylene glycol dimethyl ether electrolyte. It is evident, then, that the electrolyte plays a large role as well as that the smaller sulfur species trapped in the cathode are likely held in place by physical interactions with the carbon host.

Carbonate-based electrolytes are broadly considered to be incompatible with Li−S batteries because of the nucleophilic addition reaction between LiPS and the electrolyte, which

DOI: 10.1021/jacs.5b08113
J. Am. Chem. Soc. 2015, 137, 12143−12152

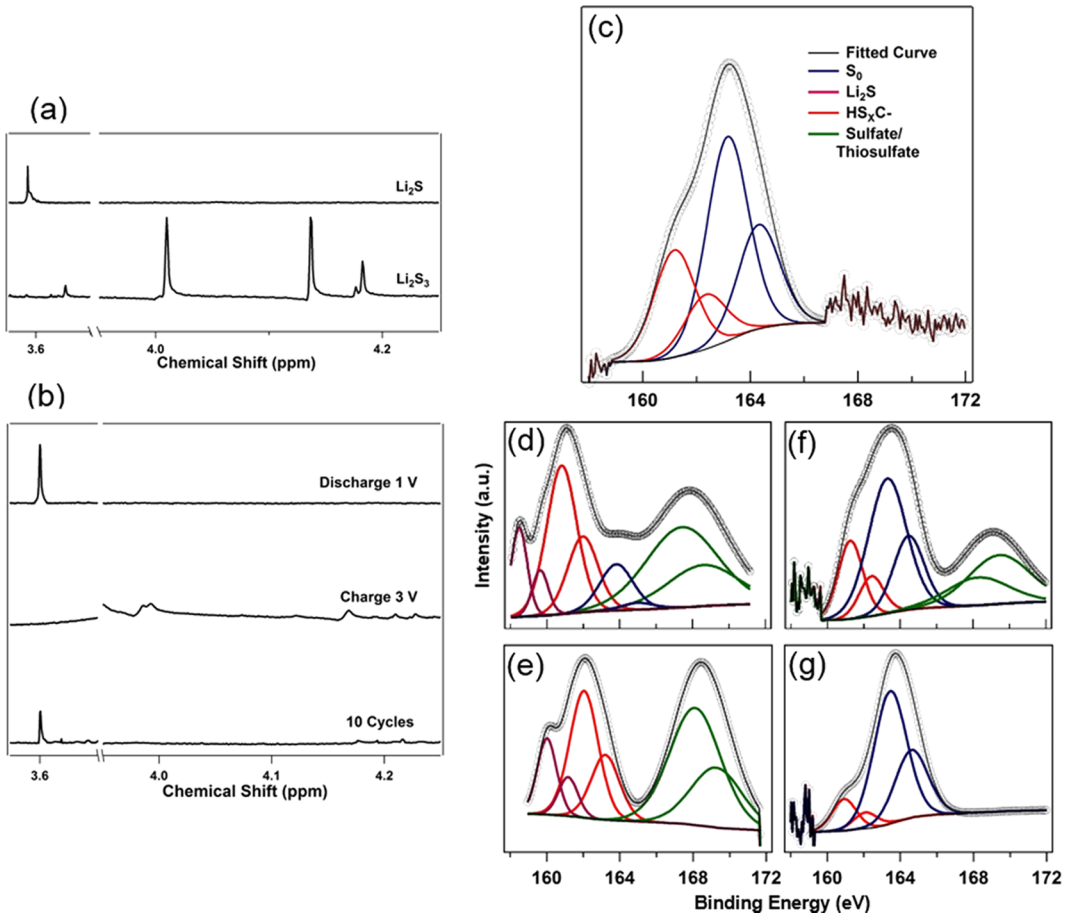

Figure 4. [1]H NMR spectra of the converted BzPS from (a) Li_2S powder and Li_2S_3 solution and (b) SPAN4 at different cycling states; ex situ XPS spectra of S 2p in SPAN4 at (c) pristine and different cycling states (cell was discharged to (d) 1.25 V and (e) 1 V, and cell was recharged to (f) 2.25 V and (g) 3 V at the first cycle, respectively).

irreversibly consumes the active sulfur in the cathode and electrolyte solvent.[43] Our finding that Li−S cells based on SPAN cathode materials cycle more stably in a carbonate-based electrolyte than in electrolytes based on DOL/DME provides additional confirmation that LiPS and its deleterious effects on carbonate electrolytes are somehow avoided when SPAN materials are used as cathodes for Li−S cells. Three hypotheses can be applied to explain these observations: (1) After the first recharge cycle, sulfur exists mainly as S_2 or S_3 in the composite and cannot form larger S_8 or reactive LiPS species in electrolyte solvents in which the smaller sulfur species or Li_2S have poor/no solubility. This would mean that Li_2S would be the only discharge product in a fully discharged cathode. (2) In the 1−3 V voltage window used, $LiNO_3$ decomposes and is irreversibly reduced on the cathode surface when the cell is discharged below 1.7 V; the minor plateau in Figure S6a would be the evidence.[44] (3) The higher solubility of LiPSs in DOL/DME promotes recombination and loss of high-order polysulfides to the electrolyte during the recharge process.[41] If this is correct, then it would confirm common, but heretofore largely untested, wisdom, namely, that an electrolyte based on a nonsolvent for LiPS with high ionic conductivity would be an ideal choice to confine sulfur in the cathode and to ensure that electrochemical reaction in the cathode occurs all in solid state.

Quantitative experiments were carried out to assess each of these hypotheses. Li_2S was either mixed with elemental sulfur or pristine SPAN4 in desired stoichiometric ratios to form a polysulfide with formula Li_2S_8. EC/DEC and DOL/DME based electrolytes were added to the LiPS species to evaluate their solubility and physical properties (photographs of the experimental setup are provided in Figure S7a). Sulfur concentrations in the resultant four solutions were recorded as a function of time using ICP-AES (Figure 3a), and UV−vis spectra of the solutions recorded after 10 days are shown in Figure 3b. It can be clearly seen that whereas sulfur is undetectable in the carbonate-based electrolyte it is readily observed in DOL/DME. Furthermore, none of the characteristic UV−vis absorption peaks associated with LiPS can be identified in the carbonate electrolyte, and no color change is noticed. In contrast, in DOL/DME, irrespective of the source of sulfur, the sulfur concentration in the electrolyte increases with time, and a color change from yellow to dark brown can be observed, which are consistent with UV−vis absorption for LiPS.[45] In the case of elemental sulfur, both sulfur concentration and LiPS absorption in UV−vis spectra are much higher than SPAN4, even at comparable sulfur loadings. It means that in the pristine SPAN electrolyte access to sulfur is limited and that SPAN4 is an effective material for sequestering LiPS. An even broader inference from these observations is that, whether the source of sulfur is SPAN or elemental sulfur, the expected polysulfide with lithium sulfide is not formed in the carbonate electrolyte solvent.

The capability of SPAN4 to hold sulfur can be indirectly assessed in a simple electrochemical measurement that reports

DOI: 10.1021/jacs.5b08113
J. Am. Chem. Soc. 2015, 137, 12143−12152

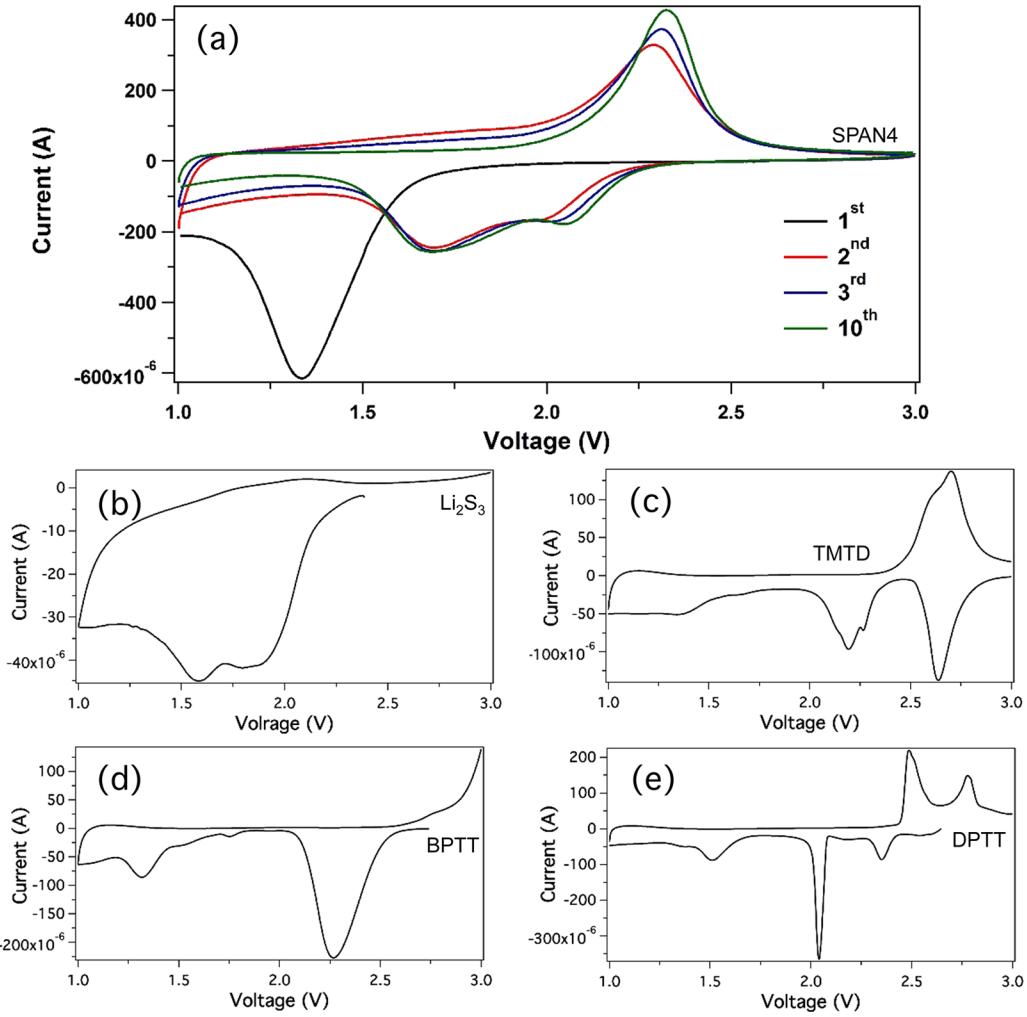

Figure 5. Cyclic voltammograms of the (a) as-prepared SPAN4 composite cathode, (b) Li_2S_3 cross-linked to PAN cathode, (c) tetramethylthiuram disulfide (TMTD) cathode, (d) bis(*p*-tolylsulfonyl) trisulfide (BPTT) cathode, (e) dipentamethylenethiuram tetrasulfide (DPTT) cathode at a scan rate of 0.1 mV/s.

the open-circuit potential (OCP) and self-discharge behavior for PAN4 and sulfur in DOL/DME (Figure S7b,c). The OCP for a cell based on elemental sulfur as the cathode is seen to gradually decrease during the 2 week time duration of the experiments. The drop in the OCP is accompanied by the LiPS dissolution and a large decrease (~53%) in capacity after 2 weeks. However, the OCP for the two cells employing cathodes based on SPAN4 shows only slight initial decreases followed by a slow stabilization toward the OCP of SPAN after 2 weeks. It suggests that the cells may need more time for the electrolyte to penetrate the separator and wet the cathode in order to reach interfacial equilibrium caused by surface tension and strain.[46] The relatively small initial decrease in capacity again suggests that even in the DOL/DME-based electrolyte SPAN4 has strong ability to hold sulfur and prevent LiPS formation and dissolution in the electrolyte. The decrease in capacity (~25%) is less than half compared to that for the elemental sulfur cathode after 2 weeks.

In order to better understand the electrochemical reactions in SPAN4 cathodes with carbonate electrolytes, the materials were studied during and post electrochemical cycling using nuclear magnetic resonance (NMR), X-ray photoelectron spectrum (XPS), Raman spectroscopy, scanning electron microscopy (SEM), and energy dispersive spectroscopy (EDS). It is known that the intermediate reaction species in Li−S cells, LiPS, are able to exist in a variety of allotrope forms due to the low energy barriers for recombination and disproportion reactions that transform higher-order LiPS to lower-order LiPS and vice versa (e.g., $Li_2S_6 \leftrightarrow 2LiS_3$).[47] Moreover, due to their atmospheric sensitivity, it is difficult to interrogate these materials using some of the most powerful chemical characterization techniques. Here, we employ an organic conversation method, wherein chemical reaction of LiPS with benzyl chloride is used to transform pure or mixed LiPS into their more stable benzyl polysulfide (BzPS) analogues without changing the order of the LiPS.[48] The high nucleophilicity of thiolate anion makes it possible to achieve nearly 100% conversion of LiPS to BzPS.[49,50] Systematic application of the method coupled with NMR analysis has been used to characterize the NMR spectra of different BzPS, allowing peak assignments to be made for different BzPS.[48,49] Figure 4a,b shows the NMR spectra obtained by reacting a mixture of DME and benzyl chloride with Li_2S powder, Li_2S_3 solution, and the cycled SPAN4 cathodes. Distinctive peak assignments for Bz_2S_3, Bz_2S_4, and Bz_2S_5 at 4.02, 4.15, and 4.20 ppm, respectively, can be found from the spectra, which are in accordance with those in previous literature.[48] A single Bz_2S peak at 3.60 ppm can be

DOI: 10.1021/jacs.5b08113
J. Am. Chem. Soc. 2015, 137, 12143−12152

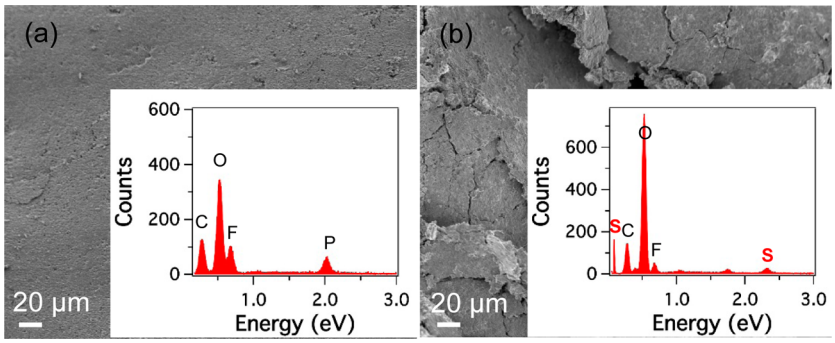

Figure 6. SEM images and EDS mapping of the lithium anode after 500 cycles in (a) EC/DEC and (b) DOL/DME based electrolytes.

found, for example, in the Li_2S case. On the other hand, the spectrum for Li_2S_3 (obtained by reacting Li_2S and S_8 in a 4:1 molar ratio) clearly shows that this material is a mixture of multiple species. On the basis of the reference spectra, we conclude that Bz_2S is the only BzPS species that exist in the discharged SPAN4 cathode. This clearly means that Li_2S is the only or the dominant discharge product in the cell. Significantly, once the cell is charged to 3 V, the chemical shift for Bz_2S disappeared and a broadened curve arises between 3.80 and 4.0 ppm, consistent with expectations for sulfur interacting/bonded to a polymeric species. After the 10th cycle of discharge, the peak for Bz_2S is seen to still exist. NMR spectra of the cathodes cycled at intermediate stages of discharge and charge are shown in Figure S10, with Bz_2S signal detected only. Our results, therefore, lend support to the hypothesis that the improved sulfur utilization of the SPAN4 cathodes is a result of the fact that elemental sulfur is fully reduced to Li_2S upon discharging. As no intermediate LiPS is found in the spectrum, it is also apparent that higher-order sulfur species do not exist in the SPAN4 composite cathode.

XPS analysis of SPAN cathodes evaluated at different states of discharge and charge provides additional insights into the electrochemical mechanisms through which these cathodes are able to achieve their exceptional cycling performance. XPS spectra in the C 1s region (Figure S8) for pristine SPAN4 reveal that the C 1s band can be split into three peaks. The main peak at 284.6 eV corresponds to the sp^2 type C−C component. The peak at 286.4 eV can be partially ascribed to the C−S or C−N bond. The minor peak at 289.3 eV represents extended delocalized electrons in the composite, resulting in a satellite structure.[34,51] Figure 4c−g presents S 2p spectra for the pristine SPAN and cathode at different galvanostatic cycling states. S 2p spectra for the pristine cathode show an overlapped band with two shoulder bands. The main S 2p 3/2 peak at 163.4 eV (Figure 4c), slightly lower than binding energy of elemental sulfur (164.0 eV), is consistent with the presence of C−S bonds in the composite. Another S 2p 3/2 peak at 161.2 eV can be attributed to adsorbed HS_xC byproduct generated in the sulfurization reaction on the surface of the composite.[12] Upon discharging (Figure 4d,e), the peaks for elemental sulfur are seen to disappear and new peaks at 168.2 eV arise from the sulfate/thiosulfate complex species, most likely formed by the oxidation of Li_2S when processing the cathode for XPS characterization.[52,53] As the peak attributed to Li_2S around 160 eV appears when discharging and disappears during charging, and no other LiPS could be found, we attribute the final discharge product in the cathode to Li_2S, which is consistent with our earlier study. We also found that peaks represent delocalized electrons in C 1s spectra increased dramatically upon discharging (Figure S8), suggesting that sulfur has an interaction with the conjugated carbon backbone during lithiation. When the cell is charged (Figure 4f,g), the oxidized sulfur peaks gradually disappear and peaks for elemental sulfur reappear, suggesting sulfur recovers to its elemental state. On the basis of the fact from the XPS C 1s (Figure S8) and Raman (Figure S9) spectra that the S−C bond recovers upon charging, we conclude that carbon in SPAN is able to reform a strong bond with sulfur.

Additional insights about the electrochemical characteristics of the SPAN4 cathodes can be deduced from cyclic voltammetry (CV). In particular, by using CV to interrogate behaviors in multiple electrochemically active sulfur compounds containing sulfur species similar to what we hypothesize to exist in the SPAN4 cells, it is possible to confirm that sulfur in the form of S_2 and S_3 is the dominant species in the cathode. In particular, Li_2S_3 cross-linked to PAN (obtained using the method reported by Guo et al.[29]) (Figure 5b), tetramethylthiuram disulfide (TMTD) (Figure 5c), bis(*p*-tolylsulfonyl) trisulfide (BPTT) (Figure 5d), or dipentamethylenethiuram tetrasulfide (DPTT) (Figure 5e) containing oligosulfides covalently linked to organic molecules was each employed as the cathode vs lithium, and their electrochemical behaviors were compared with those for SPAN4 (Figure 5a). CV curves for SPAN4 for multiple redox cycles are shown in the graph. It displays a lower plateau for the first reduction process, which agrees well with the voltage profile deduced from galvanostatic cycling studies shown Figure 2a.

It is known that organosulfur-based polymer materials with S−S linkages are capable of reversibly cleaving and reforming based on the redox chemistry of thiolates (RS^-), which can be oxidized to the corresponding radical ($RS^\bullet$) and, in turn, couple to form disulfides (RSSR).[24,35,36] This process involves one-electron transfer such that the capacity is not high compared to elemental sulfur. As these molecules contain other functional groups like thiuram and sulfonyl terminals, the reduction peaks at higher voltage can be ignored, as they are probably related to the reduction of these complex functional groups that are not related to the bond cleavage in sulfides. The reduction peaks at voltages below 2.1 V are thought to arise from S−S bond breakage, and there is a clear relation between the number of peaks in this section of the CV spectrum and the number of S−S bonds in the materials. TMTD, for example, shows one broad reduction peak at ∼1.3 V, similar to the initial reduction peak for SPAN. This suggests that, during the first discharge, the S−S bond adjacent to the carbon ring breaks in the SPAN4 composite and that it requires a higher energy input.

During cycles of discharge, the CV profile for SPAN shows similarity with that of Li_2S_3; these can be explained by sulfur

DOI: 10.1021/jacs.5b08113
J. Am. Chem. Soc. 2015, 137, 12143−12152

that detached from the carbon ring maintaining its two-electron transfer properties. A two-electron process is also consistent with the high specific capacity of this material. The absence of a similar sharp reduction peak for SPAN4 compared to that for DPTT at 2.05 V is thought to provide additional evidence that during the first discharge the S−S bond adjacent to the carbon ring breaks in the SPAN4 composite and requires a higher energy input. Thus, on the basis of these organic sulfide compound analogues, we propose that in SPAN4 electrochemically active sulfur exists principally as S_3 or S_2 attached to the adjacent carbon backbone. The complete reduction of either species is achieved in a two-electron transfer process, which is likely responsible for the high specific capacity of the material.

We close by considering the effect of a SPAN-based cathode in the Li−S cell on the metallic lithium anode. As discussed earlier, carbonate electrolytes exhibit minimum solubility for LiPS, and Li−S cells based on SPAN cathodes exhibit high Coulombic efficiency and no evidence of shuttling. We examined the morphology of lithium anodes for the Li−SPAN4 cells after 500 cycles of galvanostatic charge and discharge in both EC/DEC and DOL/DME electrolytes. Figure 6a shows the SEM image and EDS mapping of the lithium anode in carbonate electrolyte. A very dense and uniform SEI layer can be observed on the anode for cells cycled in EC/DEC electrolyte. The time-dependent growth of the SEI can explain the increase in interfacial resistance in impedance spectra (Figure S10) of the cell upon cycling, as the diffusion length is longer. This SEI can protect lithium and probably minimize lithium dendrite formation, enabling stable cycling capability. Remarkably, EDS mapping of the SEI shows no evidence of sulfur, meaning that shuttling can be eliminated when using a nonsolvent electrolyte for LiPS in the cell. Thus, complete sequestration of electrochemically active sulfur in the cathode not only facilitates complete reduction and high specific capacity but also provides a well-protected anode, which contributes the cycling stability of the Li−SPAN4 cell. The morphology of the cathode after cycling is well-maintained, and no obvious change in it can be identified from SEM images (Figure S11). However, when the cell was cycled in DOL/DME, a loose and cracked SEI was observed on the lithium anode, with abundant sulfur signal being detected (Figure 6b), explaining the shuttling phenomena in which LiPS attacks lithium metal and results in a loss of active cathode mass.

CONCLUSIONS

We have used a straightforward thermal synthesis process to create sulfur/PAN (SPAN) nanocomposites in which sulfur is so strongly linked to a conductive polymer host that its solution state electrochemistry is different from that of bulk S_8. By means of spectroscopic and electrochemical methods, we deduce that in these SPAN composites sulfur exists as S_3/S_2 units covalently attached to a carbon backbone containing pyridinic-N units. When they are used as cathodes in lithium−sulfur cells, the SPAN nanocomposites exhibit high active materials utilization, exceptional stability in extended cycling, and none of the shuttling behaviors characteristic of cathodes based on elemental sulfur. We show that the beneficial electrochemical attributes of the materials are a consequence not only of the strong interactions between sulfur and its conductive host but also the host's ability to prevent formation of S_8 after complete oxidation during recharge of the cell.

The most impressive electrochemical performance of the SPAN nanocomposite cathodes is achieved in carbonate electrolytes with minimum solubility for high-order lithium polysulfide (LiPS). In Li−SPAN cells containing these electrolytes and none of the usual salt additives (e.g., $LiNO_3$) required to stabilize the anode in conventional Li−S cells, we find no evidence of such reactions or of LiPS shuttling. We find, instead, that the electrochemical reactions between elemental sulfur in the cathode and Li ions in solution occur fully and with high efficiencies, yielding Li_2S in the solid state as the only discharge product. In contrast, Li−SPAN cells based on electrolytes containing DOL/DME solvent exhibit poor cycling, LiPS shuttling, and low efficiencies. Although more work is needed to fundamentally understand the structure evolution of sulfur in PAN during redox processes in the cathodes, our results support our hypothesis that sulfur exists stably as smaller S_2/S_3 species in the SPAN nanocomposites even after the materials are subjected to galvanostatic cycling for hundreds of cycles.

ASSOCIATED CONTENT

Supporting Information

The Supporting Information is available free of charge on the ACS Publications website at DOI: 10.1021/jacs.5b08113.

Experimental details for the preparation of the sulfur/PAN nanocomposite cathodes, materials characterization, and electrochemical analysis (PDF).

AUTHOR INFORMATION

Corresponding Author

*laa25@cornell.edu

Notes

The authors declare the following competing financial interest(s): Professor Archer is the co-founder and holds a financial interest in NOHMs Technologies, a technology concern focused on commercialization of electrodes and electrolytes for lithium−sulfur secondary batteries.

ACKNOWLEDGMENTS

The authors acknowledge support from the National Science Foundation, Partnerships for Innovation Program (grant no. IIP-1237622). Electron microscopy, X-ray diffractometry, and X-ray spectroscopy facilities and optical spectrometers available through the Cornell Center for Materials Research (CCMR) were used for this work (NSF grant no. DMR-1120296).

REFERENCES

(1) Armand, M.; Tarascon, J. M. *Nature* **2008**, *451*, 652.
(2) Bruce, P. G. *Solid State Ionics* **2008**, *179*, 752.
(3) Ji, X.; Lee, K. T.; Nazar, L. F. *Nat. Mater.* **2009**, *8*, 500.
(4) Dunn, B.; Kamath, H.; Tarascon, J.-M. *Science* **2011**, *334*, 928.
(5) Hassoun, J.; Scrosati, B. *Adv. Mater.* **2010**, *22*, 5198. Zhao, Q.; Hu, X.; Zhang, K.; Zhang, N.; Hu, Y.; Chen, J. *Nano Lett.* **2015**, *15*, 721.
(6) Whittingham, M. S. *Science* **1976**, *192*, 1126. Whittingham, M. S. *Chem. Rev.* **2004**, *104*, 4271.
(7) Gao, J.; Abruña, H. D. *J. Phys. Chem. Lett.* **2014**, *5*, 882.
(8) Manthiram, A.; Fu, Y.; Chung, S.-H.; Zu, C.; Su, Y.-S. *Chem. Rev.* **2014**, *114*, 11751.
(9) Ma, L.; Hendrickson, K. E.; Wei, S.; Archer, L. A. *Nano Today* **2015**, *10*, 315.
(10) Bruce, P. G.; Freunberger, S. A.; Hardwick, L. J.; Tarascon, J.-M. *Nat. Mater.* **2012**, *11*, 19.

DOI: 10.1021/jacs.5b08113
J. Am. Chem. Soc. 2015, 137, 12143−12152

(11) Akridge, J. R.; Mikhaylik, Y. V.; White, N. *Solid State Ionics* **2004**, *175*, 243.
(12) Fanous, J.; Wegner, M.; Grimminger, J.; Andresen, Ä.; Buchmeiser, M. R. *Chem. Mater.* **2011**, *23*, 5024. Zhang, S. S. *Energies* **2014**, *7*, 4588.
(13) Zheng, G.; Yang, Y.; Cha, J. J.; Hong, S. S.; Cui, Y. *Nano Lett.* **2011**, *11*, 4462.
(14) Zhang, C.; Wu, H. B.; Yuan, C.; Guo, Z.; Lou, X. W. *Angew. Chem., Int. Ed.* **2012**, *51*, 9592.
(15) He, G.; Ji, X.; Nazar, L. *Energy Environ. Sci.* **2011**, *4*, 2878.
(16) Zhou, W.; Xiao, X.; Cai, M.; Yang, L. *Nano Lett.* **2014**, *14*, 5250.
(17) Wu, H. B.; Wei, S.; Zhang, L.; Xu, R.; Hng, H. H.; Lou, X. W. *Chem. - Eur. J.* **2013**, *19*, 10804.
(18) Xin, S.; Gu, L.; Zhao, N. H.; Yin, Y. X.; Zhou, L. J.; Guo, Y. G.; Wan, L. J. *J. Am. Chem. Soc.* **2012**, *134*, 18510.
(19) Zhang, B.; Qin, X.; Li, G. R.; Gao, X. P. *Energy Environ. Sci.* **2010**, *3*, 1531.
(20) Wang, J.; Yang, J.; Xie, J.; Xu, N. *Adv. Mater.* **2002**, *14*, 963.
(21) Yu, X.-G.; Xie, J.-Y.; Yang, J.; Huang, H.-J.; Wang, K.; Wen, Z.-S. *J. Electroanal. Chem. Interfacial Electrochem.* **2004**, *573*, 121.
(22) Liu, Z.; Xu, Z.; Hu, X.; Gao, C. *Macromolecules* **2013**, *46*, 6931.
(23) Wei Seh, Z.; Li, W.; Cha, J. J.; Zheng, G.; Yang, Y.; McDowell, M. T.; Hsu, P.- C.; Cui, Y. *Nat. Commun.* **2013**, *4*, 1331.
(24) Burkhardt, S. E.; Conte, S.; Rodriguez-Calero, G. G.; Lowe, M. A.; Qian, H.; Zhou, W.; Gao, J.; Hennig, R. G.; Abruna, H. D. *J. Mater. Chem.* **2011**, *21*, 9553.
(25) Evers, S.; Yim, T.; Nazar, L. F. *J. Phys. Chem. C* **2012**, *116*, 19653.
(26) Hwang, D. U.S. Patent 10,719,614, May 27, 2004.
(27) Li, J.; Li, K.; Li, M.; Gosselink, D.; Zhang, Y.; Chen, P. *J. Power Sources* **2014**, *252*, 107.
(28) Zhang, Y. Z.; Liu, S.; Li, G. C.; Li, G. R.; Gao, X. P. *J. Mater. Chem. A* **2014**, *2*, 4652.
(29) Guo, J.; Yang, Z.; Yu, Y.; Abruña, H. D.; Archer, L. A. *J. Am. Chem. Soc.* **2013**, *135*, 763.
(30) Ma, L.; Zhuang, H.; Lu, Y.; Moganty, S. S.; Hennig, R. G.; Archer, L. A. *Adv. Energy Mater.* **2014**, *4*, 1400390.
(31) Wang, J.; Yang, J.; Wan, C.; Du, K.; Xie, J.; Xu, N. *Adv. Funct. Mater.* **2003**, *13*, 487.
(32) Yin, L.; Wang, J.; Lin, F.; Yang, J.; Nuli, Y. *Energy Environ. Sci.* **2012**, *5*, 6966.
(33) Hwang, T. H.; Jung, D. S.; Kim, J.-S.; Kim, B. G.; Choi, J. W. *Nano Lett.* **2013**, *13*, 4532.
(34) Luo, C.; Zhu, Y.; Wen, Y.; Wang, J.; Wang, C. *Adv. Funct. Mater.* **2014**, *24*, 4082.
(35) Liu, M.; Visco, S. J.; De Jonghe, L. C. *J. Electrochem. Soc.* **1989**, *136*, 2570.
(36) Kiya, Y.; Iwata, A.; Sarukawa, T.; Henderson, J. C.; Abruña, H. D. *J. Power Sources* **2007**, *173*, 522.
(37) Yu, X.; Xie, J.; Li, Y.; Huang, H.; Lai, C.; Wang, K. *J. Power Sources* **2005**, *146*, 335.
(38) Wang, L.; He, X.; Li, J.; Gao, J.; Guo, J.; Jiang, C.; Wan, C. *J. Mater. Chem.* **2012**, *22*, 22077.
(39) Wang, L.; He, X.; Sun, W.; Li, J.; Gao, J.; Tian, G.; Wang, J.; Fan, S. *RSC Adv.* **2013**, *3*, 3227.
(40) Barchasz, C.; Molton, F.; Duboc, C.; Leprêtre, J.-C.; Patoux, S.; Alloin, F. *Anal. Chem.* **2012**, *84*, 3973.
(41) Cuisinier, M.; Hart, C.; Balasubramanian, M.; Garsuch, A.; Nazar, L. F. *Adv. Energy Mater.* **2015**, *5*, 1401801.
(42) Park, H.; Koh, H. S.; Siegel, D. J. *J. Phys. Chem. C* **2015**, *119*, 4675.
(43) Yim, T.; Park, M.-S.; Yu, J.-S.; Kim, K. J.; Im, K. Y.; Kim, J.-H.; Jeong, G.; Jo, Y. N.; Woo, S.-G.; Kang, K. S.; Lee, I.; Kim, Y.-J. *Electrochim. Acta* **2013**, *107*, 454.
(44) Su, Y.-S.; Fu, Y.; Cochell, T.; Manthiram, A. *Nat. Commun.* **2013**, *4*, 2985.
(45) Suo, L.; Hu, Y.-S.; Li, H.; Armand, M.; Chen, L. *Nat. Commun.* **2013**, *4*, 1481.
(46) Sondag-Huethorst, J. A. M.; Fokkink, L. G. J. *Langmuir* **1992**, *8*, 2560.
(47) Rauh, R. D.; Shuker, F. S.; Marston, J. M.; Brummer, S. B. *J. Inorg. Nucl. Chem.* **1977**, *39*, 1761. Manan, N. S. A.; Aldous, L.; Alias, Y.; Murray, P.; Yellowlees, L. J.; Lagunas, M. C.; Hardacre, C. *J. Phys. Chem. B* **2011**, *115*, 13873.
(48) Kawase, A.; Shirai, S.; Yamoto, Y.; Arakawa, R.; Takata, T. *Phys. Chem. Chem. Phys.* **2014**, *16*, 9344.
(49) Yamada, N.; Furukawa, M.; Nishi, M.; Takata, T. *Chem. Lett.* **2002**, *31*, 454.
(50) Takata, T.; Saeki, D.; Makita, Y.; Yamada, N.; Kihara, N. *Inorg. Chem.* **2003**, *42*, 3712.
(51) Ye, J.; He, F.; Nie, J.; Cao, Y.; Yang, H.; Ai, X. *J. Mater. Chem. A* **2015**, *3*, 7406.
(52) Yang, C.-P.; Yin, Y.-X.; Guo, Y.-G.; Wan, L.-J. *J. Am. Chem. Soc.* **2015**, *137*, 2215.
(53) Hendrickson, K. E.; Ma, L.; Cohn, G.; Lu, Y.; Archer, L. A. *Adv. Sci.* **2015**, *2*, 1500068.

DOI: 10.1021/jacs.5b08113
J. Am. Chem. Soc. 2015, 137, 12143−12152